

Lineshape of the $\Lambda(1405)$ Hyperon Measured Through its $\Sigma^0\pi^0$ Decay

I. Zychor^a, M. Büscher^b, M. Hartmann^b, A. Kacharava^{c,d},
I. Keshelashvili^{b,c}, A. Khoukaz^e, V. Kleber^f, V. Koptev^g,
Y. Maeda^h, T. Mersmann^e, S. Mikirtychiants^g, R. Schleichert^b,
H. Ströher^b, Yu. Valdau^g, C. Wilkin^{i,*}

^a*The Andrzej Soltan Institute for Nuclear Studies, 05-400 Świerk, Poland*

^b*Institut für Kernphysik, Forschungszentrum Jülich, 52425 Jülich, Germany*

^c*High Energy Physics Institute, Tbilisi State University, 0186 Tbilisi, Georgia*

^d*Physikalisches Institut II, Universität Erlangen-Nürnberg, 91058 Erlangen, Germany*

^e*Institut für Kernphysik, Universität Münster, 48149 Münster, Germany*

^f*Physikalisches Institut, Universität Bonn, 53115 Bonn, Germany*

^g*High Energy Physics Department, Petersburg Nuclear Physics Institute, 188350 Gatchina, Russia*

^h*Research Center for Nuclear Physics, Osaka University, Ibaraki, Osaka 567-0047, Japan*

ⁱ*Physics and Astronomy Department, UCL, London, WC1E 6BT, UK*

Abstract

The $pp \rightarrow pK^+Y^0$ reaction has been studied for hyperon masses $m(Y^0) \leq 1540$ MeV/ c^2 at COSY-Jülich by using a 3.65 GeV/ c circulating proton beam incident on an internal hydrogen target. Final states comprising two protons, one positively charged kaon and one negatively charged pion have been identified with the ANKE spectrometer. Such configurations are sensitive to the production of the ground state Λ and Σ^0 hyperons as well as the $\Sigma^0(1385)$ and $\Lambda(1405)$ resonances. Applying invariant- and missing-mass techniques, the two overlapping excited states could be well separated, though with limited statistics. The shape and position of the $\Lambda(1405)$ distribution, reconstructed cleanly in the $\Sigma^0\pi^0$ channel, are similar to those found from other decay modes and there is no obvious mass shift. This finding constitutes a challenging test for models that predict $\Lambda(1405)$ to be a two-state resonance.

Key words: Hyperon resonances, line shapes

PACS: 14.20.Jn, 13.30.-a

The excited states of the nucleon are a topical field of research, since the full spectrum contains deep-rooted information about the underlying strong colour force acting between the quarks and gluons. In addition to searching for missing resonances predicted by quark models [1], it is important to understand the structure of certain well established states, such as the $\Lambda(1405)$ hyperon resonance.

Although a four–star resonance [2], and known already for many years, the dynamics of the $\Lambda(1405)$ are still not fully understood. Within the quark model it can be explained as a P –wave q^3 baryon [3]. It is also widely discussed as a candidate for a $\bar{K}N$ molecular state [4], or for one with a more intrinsic $q^4\bar{q}$ pentaquark structure [5]. If the $\Lambda(1405)$ is a dynamically generated resonance produced *via* $\bar{K}N$ rescattering within a coupled–channel formalism [6,7], it may consist of two overlapping $I = 0$ states [8,9,10]. Its decay spectrum would then depend upon the production reaction. Due to the opening of the $\bar{K}N$ channels, the $\Lambda(1405)$ lineshape is not represented satisfactorily by a Breit–Wigner resonance [4,11,12,13]. Nevertheless, if the $\Lambda(1405)$ were a single quantum state, as in the quark model or molecular pictures, its lineshape should be independent of the production method.

Part of the difficulty in elucidating the nature of the $\Lambda(1405)$ is due to it overlapping the nearby $\Sigma^0(1385)$. The interference between these two states can distort significantly the $\Sigma^+\pi^-$ and $\Sigma^-\pi^+$ spectra [6], for which there are experimental indications [14]. This interference can be eliminated by taking the average of $\Sigma^+\pi^-$ and $\Sigma^-\pi^+$ data [11] but the cleanest approach is through the measurement of the $\Sigma^0\pi^0$ channel, since isospin forbids this for $\Sigma^0(1385)$ decay. This is the technique that we want to develop here and, although our statistics are rather poor, these are already sufficient to yield promising results.

We have used data obtained during high statistics ϕ –production measurements with the ANKE spectrometer [15] to study the excitation and decay of low–lying hyperon resonances in pp collisions at a beam momentum of 3.65 GeV/c in an internal–ring experiment at COSY–Jülich. A dense hydrogen cluster–jet gas target was used and over a four–week period this yielded an integrated luminosity of $L = (69 \pm 10) \text{ pb}^{-1}$, as determined from elastic pp scattering that was measured in parallel and compared with the SAID 2004 solution [16].

The detection systems of the magnetic three–dipole spectrometer ANKE simultaneously register and identify both negatively and positively charged particles [17]. Forward (Fd) and side–wall (Sd) counters were used for protons, telescopes and side–wall scintillators for K^+ , and scintillators for π^- . Since the efficiencies of the detectors are constant to 2% (σ) across the momentum range of registered particles, any uncertainty in this can be neglected in the

* Corresponding author.

Email address: cw@hep.ucl.ac.uk (C. Wilkin).

further analysis.

The basic principle of the experiment is the search for four-fold coincidences, comprising two protons, one positively charged kaon and one negatively charged pion, i.e., $pp \rightarrow pK^+p\pi^-X^0$. Such a configuration can correspond, e.g., to the following reaction chains involving the $\Sigma^0(1385)$ and $\Lambda(1405)$ as intermediate states:

- (1) $pp \rightarrow pK^+\Sigma^0(1385) \rightarrow pK^+\Lambda\pi^0 \rightarrow pK^+p\pi^-\pi^0$
- (2) $pp \rightarrow pK^+\Lambda(1405) \rightarrow pK^+\Sigma^0\pi^0 \rightarrow pK^+\Lambda\gamma\pi^0 \rightarrow pK^+p\pi^-\gamma\pi^0$.

In the $\Sigma^0(1385)$ case, the residue is $X^0 = \pi^0$, while for the $\Lambda(1405)$, $X^0 = \pi^0\gamma$. The resonances overlap significantly because the widths of $36 \text{ MeV}/c^2$ for $\Sigma^0(1385)$ and $50 \text{ MeV}/c^2$ for $\Lambda(1405)$ are much larger than the mass difference [2]. The strategy to discriminate between them is to: (i) detect and identify four charged particles p_{Fd} , p_{Sd} , K^+ and π^- in coincidence, thereby drastically reducing the accidental background at the expense of statistics, (ii) select those events for which the mass of a $(p_{Sd}\pi^-)$ pair corresponds to that of the Λ , (iii) select the mass of the residue $m(X^0)$ to be that of the π^0 to tag the $\Sigma^0(1385)$, and $m(X^0) > m(\pi^0) + 55 \text{ MeV}/c^2$ for the $\Lambda(1405)$.

Figure 1a shows the two-dimensional distribution of the four-particle missing mass $MM(pK^+\pi^-p)$ of the $p_{Sd}\pi^-$ pairs *versus* the invariant mass $M(p_{Sd}\pi^-)$. A vertical band corresponding to the Λ , is visible around a mass of $1116 \text{ MeV}/c^2$. The features of this band are illustrated clearly in the projection onto the $M(p_{Sd}\pi^-)$ axis shown in Fig. 1b. The Λ peak, with a FWHM of $\sim 5 \text{ MeV}/c^2$, sits on a slowly varying background, much of which arises from a false $p\pi^-$ association (the combinatorial background).

Data within the invariant-mass window $1112\text{--}1120 \text{ MeV}/c^2$ were retained for further analysis and, in Fig. 2, $MM(p_{Fd}K^+)$ is plotted against $MM(pK^+p\pi^-)$ for these events. The triangular-shaped domain arises from the constraint $MM(p_{Fd}K^+) \geq MM(pK^+p\pi^-) + m(\Lambda)$. Despite the lower limit of $50 \text{ MeV}/c^2$ on $MM(pK^+p\pi^-)$, there is a background from Σ^0 production at the bottom of the triangle, but this can be easily cut away. The enhancement for $MM(p_{Fd}K^+) \sim 1400 \text{ MeV}/c^2$ corresponds to $\Sigma^0(1385)$ and $\Lambda(1405)$ production. The two vertical bands show the four-particle missing-mass $MM(pK^+p\pi^-)$ criteria used to separate the $\Sigma^0(1385)$ from the $\Lambda(1405)$. The left band is optimised to identify a π^0 whereas, in view of the missing-mass resolution, the right one selects masses significantly greater than $m(\pi^0)$.

Since the properties of the $\Sigma^0(1385)$ are undisputed [2], we first present and discuss results for this hyperon as a test case for the $\Lambda(1405)$ analysis. In Fig. 3 we show the experimental missing-mass $MM(p_{Fd}K^+)$ spectrum for

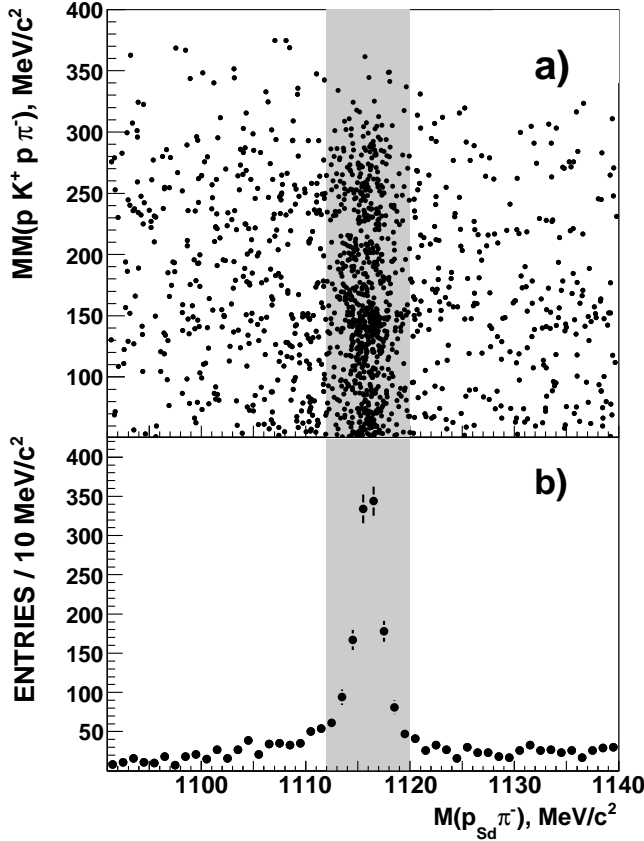


Fig. 1. a) Missing mass $MM(pK^+p\pi^-)$ versus invariant mass $M(p_{Sd}\pi^-)$. The shaded vertical box shows the band used to select the Λ . b) The projection of all the events from panel a) onto the $M(p_{Sd}\pi^-)$ axis shows a clear Λ peak with a FWHM projection of $\sim 5 \text{ MeV}/c^2$ and a slowly varying background.

events within the π^0 -band of Fig. 2. When this is fit with a Breit–Wigner distribution plus a linear background, a mass of $M = (1384 \pm 10) \text{ MeV}/c^2$ and a width of $\Gamma \sim 40 \text{ MeV}/c^2$ are obtained, in good agreement with the PDG values [2]. The resonance is located half way between the $\Sigma\pi$ and $\bar{K}N$ thresholds, indicated by arrows in Fig. 3, and no significant influence of either threshold is observed in the data.

To investigate possible contributions to the spectrum other than from the $\Sigma^0(1385)$ excitation, Monte Carlo simulations were performed for backgrounds from non-resonant and resonant production. The first group of reactions includes processes such as $pp \rightarrow NK^+\pi X(\gamma)$ and $pp \rightarrow NK^+\pi\pi X(\gamma)$, with X

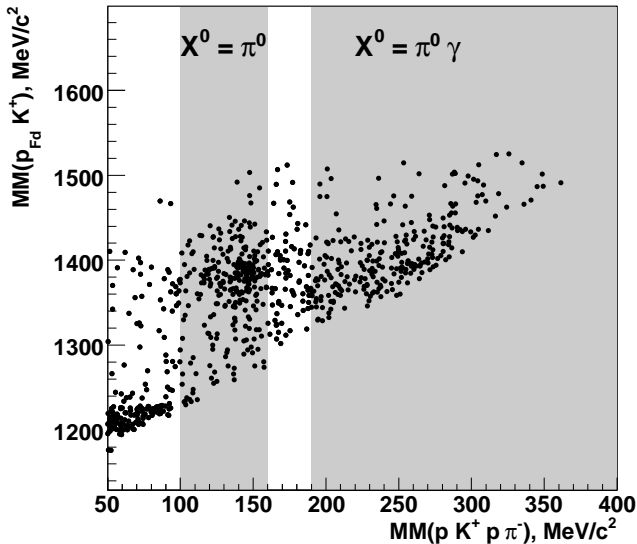


Fig. 2. Missing mass $MM(p_{Fd}K^+)$ versus $MM(pK^+p\pi^-)$. A clear concentration of π^0 events is seen, though with a central value of the mass $\sim 8\text{ MeV}/c^2$ too high, a deviation that is consistent with the resolution expected for a four-particle missing mass. The left shaded vertical box covers this π^0 region and the right one has $MM(pK^+p\pi^-) > 190\text{ MeV}/c^2$ originating, e.g., from $\pi^0\gamma$ and $\pi\pi$.

representing any allowed Λ or Σ hyperon. The second group comprises $\Lambda(1405)$ and $\Lambda(1520)$ hyperon production. The simulations, based on the GEANT3 package, were performed in a similar manner to those in Ref. [18]. Events were generated according to phase space using relativistic Breit–Wigner parametrisations for the known hyperon resonances [2]. Their relative contributions were deduced by fitting the experimental data, giving the results shown by the histograms of Fig. 3. Also included is a small contribution from the $\Lambda(1405)$ channel, arising from the tail of the missing-mass events in Fig. 2 leaking into the π^0 region. As expected, the $\Sigma^0(1385)$ peak dominates over a small and smooth background.

In order to estimate the total $\Sigma^0(1385)$ production cross section we used the overall detector efficiency of $\sim 55\%$ and the cumulative branching ratio of 56% for the $\Sigma^0(1385)$ decay chain corresponding to reaction (1). With the calculated acceptance of $\sim 2 \times 10^{-6}$ and the number of $\Sigma^0(1385)$ events equal to 170 ± 26 , we find

$$\sigma_{\text{tot}}(pp \rightarrow pK^+\Sigma^0(1385)) = (4.0 \pm 1.0_{\text{stat}} \pm 1.6_{\text{syst}}) \mu\text{b}.$$

at $p_{\text{beam}} = 3.65\text{ GeV}/c$. The systematic uncertainty in the fitting procedure and cross section evaluation was estimated by varying some of the event selection parameters, such as the width of the $MM(pK^+p\pi^-)$ bands or the range

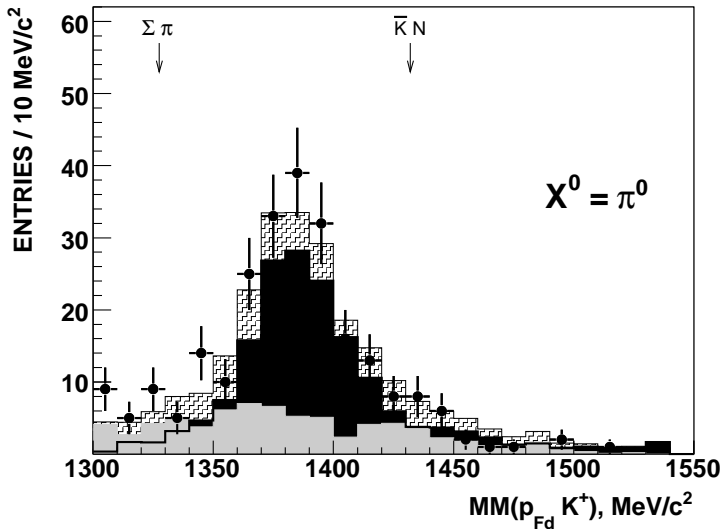


Fig. 3. Missing-mass $MM(p_{Fd}K^+)$ distribution for the $pp \rightarrow pK^+p\pi^- X^0$ reaction for events with $M(p_{Sd}\pi^-) \approx m(\Lambda)$ and for $MM(pK^+p\pi^-) \approx m(\pi^0)$. Experimental points with statistical errors are compared to the shaded histogram of the fitted overall Monte Carlo simulations. The simulation includes resonant contributions (solid-black) and non-resonant phase-space production (solid-grey). The structure in the latter arises from the various channels considered. Arrows indicate the $\Sigma\pi$ and $\bar{K}N$ thresholds.

for the Λ peak (see Fig. 1), or the non-resonant background in Fig. 3. The cross section is only a little lower than at 6 GeV/c, $(7 \pm 1) \mu\text{b}$ [19], whereas that for $pp \rightarrow pK^+\Lambda$ increases by a factor of four over a similar change in excess energy [20].

Turning now to the $\Lambda(1405)$, simulations show that the $\Sigma^0(1385)$ does not contaminate the missing-mass $MM(pK^+p\pi^-)$ range above 190 MeV/c². This point is crucial since it allows us to obtain a clean separation of the $\Sigma^0(1385)$ and $\Lambda(1405)$. There is the possibility of some contamination from the $pK^+\Lambda(\pi\pi)^0$ channel but there is only a limited amount of the five-body phase space available near the maximum missing mass. Simulations also show that the ANKE acceptance varies only marginally in the mass range around 1400 MeV/c². The corresponding experimental missing-mass $MM(p_{Fd}K^+)$ spectrum is shown in Fig. 4a. The asymmetric distribution, which peaks around 1400 MeV/c², has a long tail on the high missing-mass side that extends up to the kinematical limit.

In order to extract the $\Lambda(1405)$ distribution from the measured $\Sigma^0\pi^0$ decay, a different strategy has been applied, where we first fit the non-resonant contributions to the experimental data. The fit was performed for $1440 < MM(p_{Fd}K^+) < 1490$ MeV/c² to exclude heavier hyperon resonances, such

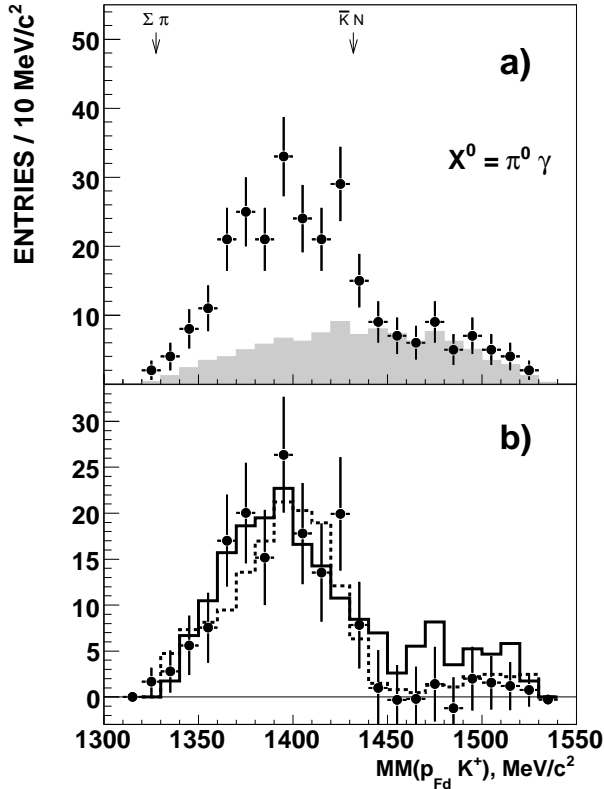


Fig. 4. a) Missing-mass $MM(p_{Fd}K^+)$ distribution for the $pp \rightarrow pK^+p\pi^-X^0$ reaction for events with $M(p_{Sd}\pi^-) \approx m(\Lambda)$ and $MM(pK^+p\pi^-) > 190 \text{ MeV}/c^2$. Experimental points with statistical errors are compared to the shaded histogram of the fitted non-resonant Monte Carlo simulation. b) The background-subtracted line-shape of the $\Lambda(1405)$ decaying into $\Sigma^0\pi^0$ (points) compared to $\pi^-p \rightarrow K^0(\Sigma\pi)^0$ [13] (solid line) and $K^-p \rightarrow \pi^+\pi^-\Sigma^+\pi^-$ [11] (dotted line) data.

as the $\Lambda(1520)$. The resulting non-resonant background is indicated by the shaded histogram in Fig. 4a. When this is subtracted from the data we obtain the distribution shown as experimental points in Fig. 4b.

Our background-subtracted data exhibit a prominent structure around $1400 \text{ MeV}/c^2$. There is no indication of a second near $1500 \text{ MeV}/c^2$, which might result from the production of the $\Lambda(1520)$ [11]. The excess of at most 20 events for $MM(p_{Fd}K^+) > 1490 \text{ MeV}/c^2$ leads to an upper limit for the $\Lambda(1520)$ production cross section of $\sigma_{\text{tot}} < 0.2 \mu\text{b}$. The smallness of the signal in this case would be largely due to the low branching of only 9% into this channel. There is no evidence either for a significant contribution from the $Y^{0*}(1480)$ hyperon [18]. If this state were the same as the one-star $\Sigma^0(1480)$ of Ref.[2],

the decay into $\Sigma^0\pi^0$ would be forbidden. However, this state is also not seen in the $K^-p \rightarrow \pi^0\pi^0\Lambda$ reaction [21].

We finally turn to the contribution from lower missing masses. From the number of events with $1320 < MM(p_{Fd}K^+) < 1440 \text{ MeV}/c^2$, equal to 156 ± 23 , we find a total production cross section of

$$\sigma_{\text{tot}}(pp \rightarrow pK^+\Lambda(1405)) = (4.5 \pm 0.9_{\text{stat}} \pm 1.8_{\text{syst}}) \mu\text{b}$$

at $p_{\text{beam}} = 3.65 \text{ GeV}/c$. The cumulative branching ratio for the $\Lambda(1405)$ decay chain of reaction (2) of 21% and the acceptance of $\sim 4 \times 10^{-6}$ have been included, as well as the overall detection efficiency of $\sim 55\%$.

The $(\Sigma\pi)^0$ invariant-mass distributions have been studied in two hydrogen bubble chamber experiments. Thomas *et al.* [13] found ~ 400 $\Sigma^+\pi^-$ or $\Sigma^-\pi^+$ events corresponding to the $\pi^-p \rightarrow K^0\Lambda(1405) \rightarrow K^0(\Sigma\pi)^0$ reaction at a beam momentum of $1.69 \text{ GeV}/c$. Hemingway [11] used a $4.2 \text{ GeV}/c$ kaon beam to investigate $K^-p \rightarrow \Sigma^+(1660)\pi^- \rightarrow \Lambda(1405)\pi^+\pi^- \rightarrow (\Sigma^\pm\pi^\mp)\pi^+\pi^-$. For the $\Sigma^-\pi^-\pi^+\pi^+$ final state, the $\Sigma^-\pi^+$ mass spectrum is distorted by the confusion between the two positive pions. Thus, in the comparison with our data, we use only the $\Sigma^+\pi^-$ distribution, which contains 1106 events [11].

In Fig. 4b our experimental points are compared to the results of Thomas and Hemingway, which have been normalised by scaling their values down by factors of ~ 3 and ~ 7 , respectively. The effect of the $\bar{K}N$ threshold is apparent in these published data, with the $\Lambda(1405)$ mass distribution being distorted by the opening of this channel. Despite the very different production mechanisms, the three distributions have consistent shapes. A fit of one to either of the others leads to a χ^2/ndf of the order of unity though, as pointed out in Ref. [6], for $\Sigma^+\pi^-$ production [11] there is likely to be some residual distortion from $I = 1$ channels. The $K^-p \rightarrow \Lambda(1405)\pi^0 \rightarrow \Sigma^0\pi^0\pi^0$ data yield a somewhat different distribution [22] but, as noted in this reference, the uncertainty as to which π^0 originated from the $\Lambda(1405)$ “*smears the resonance signal in the spectra*”. The situation is therefore very similar to that of the Hemingway $\Sigma^-\pi^-\pi^+\pi^+$ data [11] and such results can only be interpreted within the context of a specific reaction model, such as that of Ref. [9].

Models based on unitary chiral perturbation theory find two poles in the neighborhood of the $\Lambda(1405)$ which evolve from a singlet and an octet in the exact $SU(3)$ limit [8,9]. One has a mass of $1390 \text{ MeV}/c^2$ and a width of $130 \text{ MeV}/c^2$ and couples preferentially to $\Sigma\pi$. The narrower one, located at $1425 \text{ MeV}/c^2$, couples more strongly to $\bar{K}N$, whose threshold lies at $\sim 1432 \text{ MeV}/c^2$. Both states may contribute to the experimental distributions, and it is their relative population, which depends upon the production mechanism, that will determine the observed lineshape. Our experimental findings show that the

properties (mass, width, and shape) of the $\Lambda(1405)$ resonance are essentially identical for these three different production modes.

In summary, we have measured the excitation of the $\Sigma^0(1385)$ and $\Lambda(1405)$ hyperon resonances in proton–proton collisions at a beam momentum of 3.65 GeV/c. We have succeeded in unambiguously separating the two states through their $\Lambda\pi^0$ and $\Sigma^0\pi^0 \rightarrow \Lambda\gamma\pi^0$ decay modes. Cross sections of the order of a few μb have been deduced for both resonances. The $\Lambda(1405)$, as measured through its $\Sigma^0\pi^0$ decay, has a shape that is consistent with data on the charged decays [11,13], with a mass of $\sim 1400 \text{ MeV}/c^2$ and width of $\sim 60 \text{ MeV}/c^2$. This might suggest that, if there are two states present in this region, then the reaction mechanisms in the three cases are preferentially populating the same one. However, by identifying particular reaction mechanisms, proponents of the two–state solution can describe the shape of the distribution that we have found [10].

The $\Sigma^0\pi^0$ channel is by far the cleanest for the observation of the $\Lambda(1405)$ since it is not contaminated by the $\Sigma(1385)$ nor the confusion regarding the identification of the pion from its decay. However, although we have shown that the method works in practice, in view of our limited statistics, further data are clearly needed. The decay $\Lambda(1405) \rightarrow \Sigma^0\pi^0 \rightarrow \Lambda\gamma\pi^0$ can be detected directly in electromagnetic calorimeters. Corresponding measurements are under way in γp reactions (CB/TAPS at ELSA [23], SPring–8/LEPS [24]) and are also planned in pp interactions with WASA at COSY [25].

We acknowledge many very useful discussions with E. Oset. We also thank all other members of the ANKE collaboration and the COSY accelerator staff for their help during the data taking. This work has been supported by COSY-FFE Grant, BMBF, DFG and Russian Academy of Sciences.

References

- [1] S. Capstick and W. Roberts, *Prog. Part. Nucl. Phys.* **45** (2000) S241.
- [2] W.-M. Yao et al., *J. Phys. G* **33** (2006) 1, but see also the minireview in D.E. Groom et al., *Eur. Phys. J. C* **15** (2000) 1.
- [3] N. Isgur and G. Karl, *Phys. Rev. D* **18** (1978) 4187.
- [4] R.H. Dalitz and S.F. Tuan, *Ann. Phys. (N.Y.)* **10** (1960) 307.
- [5] T. Inoue, *Nucl. Phys. A* **790** (2007) 530.
- [6] J.C. Nacher, et al., *Phys. Lett. B* **455** (1999) 55.
- [7] J.A. Oller and Ulf-G. Meißner, *Phys. Lett. B* **500** (2001) 263.

- [8] D. Jido et al., Nucl. Phys. A **725** (2003) 181.
- [9] V.K. Magas, E. Oset and A. Ramos, Phys. Rev. Lett. **95** (2005) 052301.
- [10] L.S. Geng and E. Oset, arXiv:0707.3343 [hep-ph].
- [11] R.J. Hemingway, Nucl. Phys. B **253** (1984) 742.
- [12] R.H. Dalitz and A. Deloff, J. Phys. G **17** (1991) 289.
- [13] D.W. Thomas, et al., Nucl. Phys. B **56** (1973) 15.
- [14] J.K. Ahn, Nucl. Phys. A **721** (2003) 715c.
- [15] M. Hartmann et al., COSY Proposal # 104,
www.fz-juelich.de/ikp/anke/en/proposals.shtml (2002).
- [16] R.A. Arndt, I.I. Strakovsky, and R.L. Workman, Phys. Rev. C **62** (2000) 034005;
<http://gwadc.phys.gwu.edu>, SAID solution **SP04**.
- [17] S. Barsov et al., Nucl. Instr. Meth. A **462** (2001) 364.
- [18] I. Zychor et al., Phys. Rev. Lett. **96** (2006) 012002.
- [19] S. Klein et al., Phys. Rev. D **1** (1970) 3019.
- [20] A. Sibirtsev et al., Eur. Phys. J. A **29** (2006) 363.
- [21] S. Prakhov et al., Phys. Rev. C **69** (2004) 042202(R).
- [22] S. Prakhov et al., Phys. Rev. C **70** (2004) 034605.
- [23] H. Schmieden, ELSA Letter of Intent ELSA/4-2003.
- [24] H. Fujimura, AIP Conf. Proc. **915** (2007) 737.
- [25] H.-H. Adam et al., nucl-ex/0411038.